Supporting Information

Synthesis and electrochemical properties of spherical and hollow-structured NiO aggregates created by combining the Kirkendall effect and Ostwald ripening

*Jung Sang Cho, Jong Min Won, Jong-Heun Lee, and Yun Chan Kang**

Department of Materials Science and Engineering
Korea University
Anam-Dong, Seongbuk-Gu
Seoul 136-713, Republic of Korea
E-mail: *yckang@korea.ac.kr*

Keywords: Kirkendall diffusion; Ostwald ripening; nanopowders; nickel oxide; lithium ion battery; spray pyrolysis

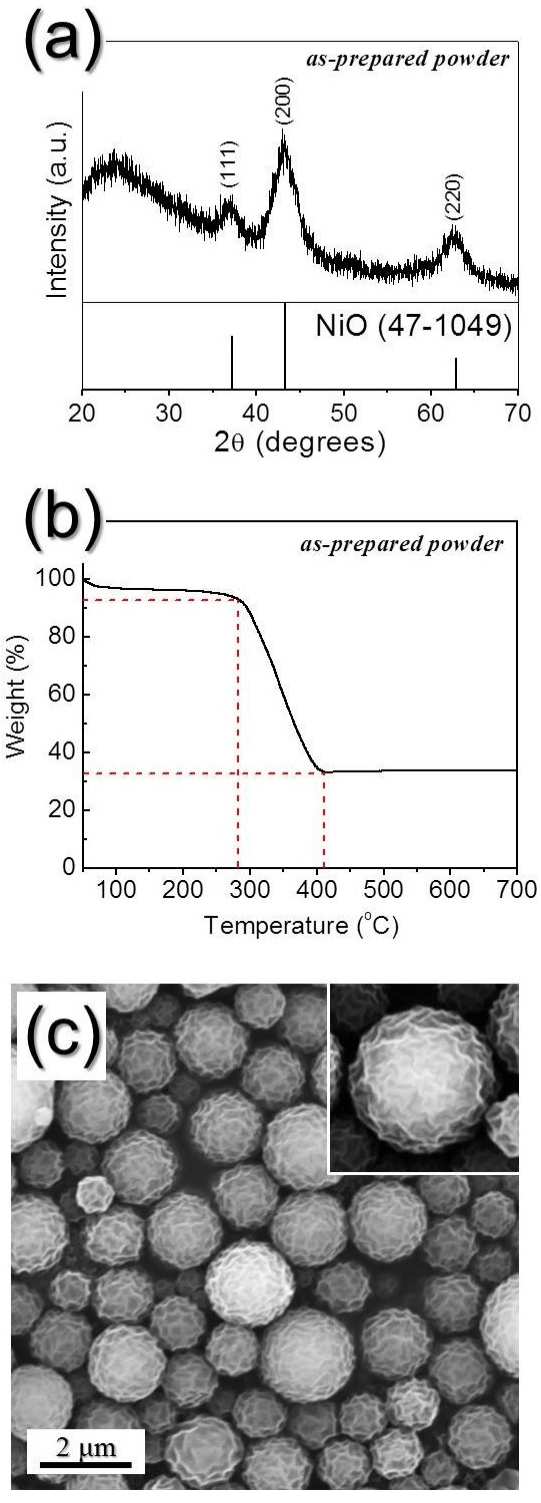

Fig. S1 (a) XRD pattern, (b) TG curve, and (c) SEM image of the as-prepared precursor powders directly obtained by spray pyrolysis process.

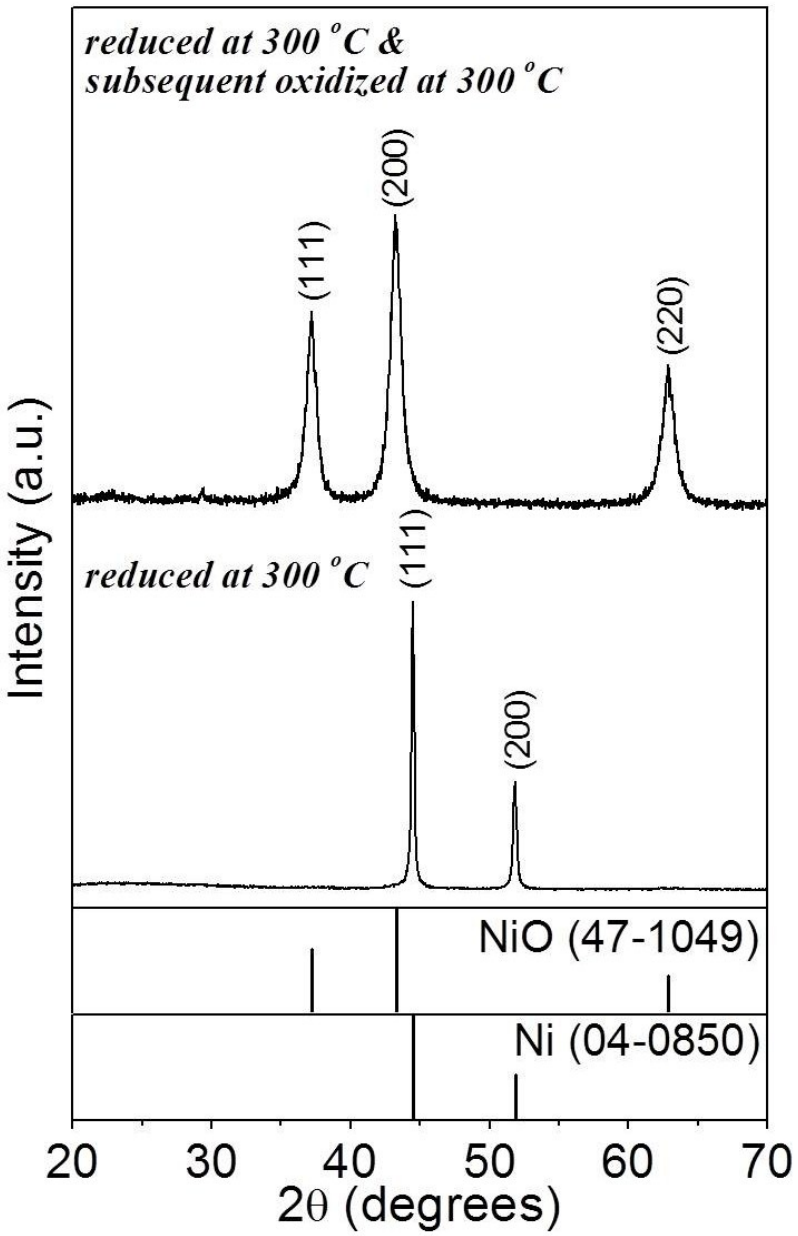

Fig. S2. XRD patterns of the Ni-C composite powders obtained by reduction process at 300 °C under 10% H_2/Ar gas and hollow NiO aggregates obtained by oxidation of the reduced Ni-C composite powders at 300 °C under air.

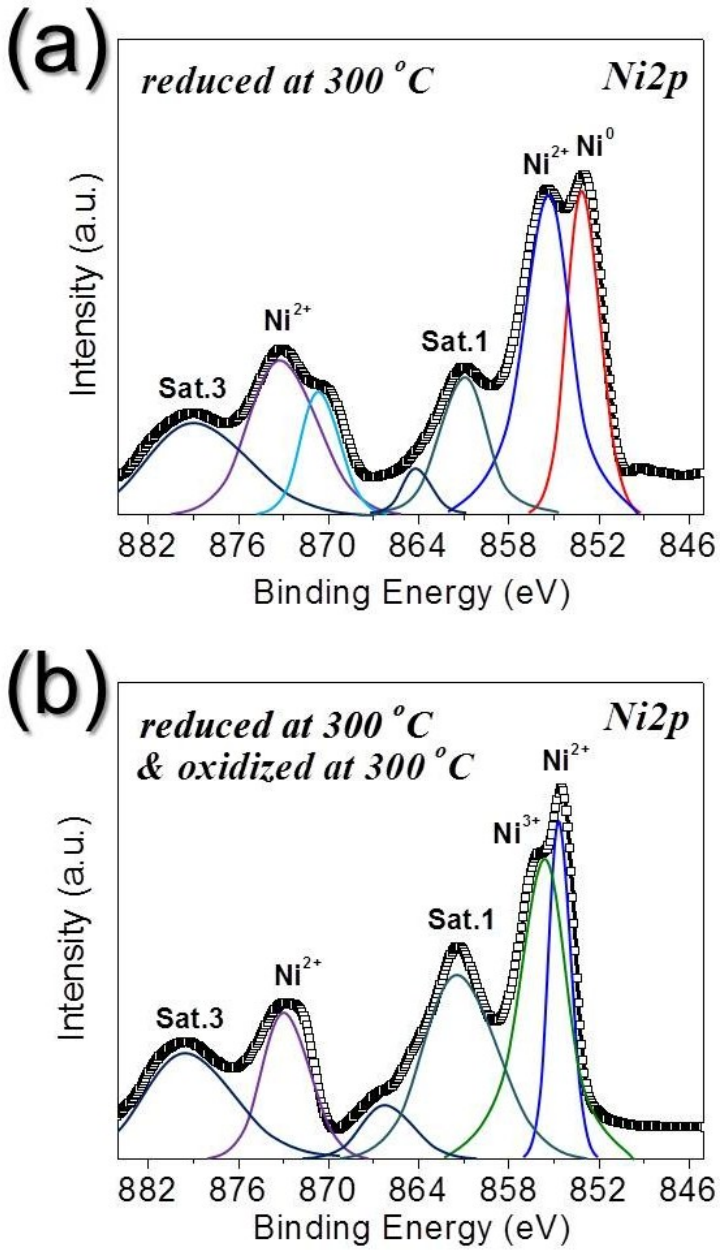

Fig. S3. Ni2p XPS spectra of the (a) Ni-C composite powders obtained by reduction process at 300 °C under 10% H_2/Ar gas and (b) hollow NiO aggregates obtained by oxidation of the reduced Ni-C composite powders at 300 °C under air.

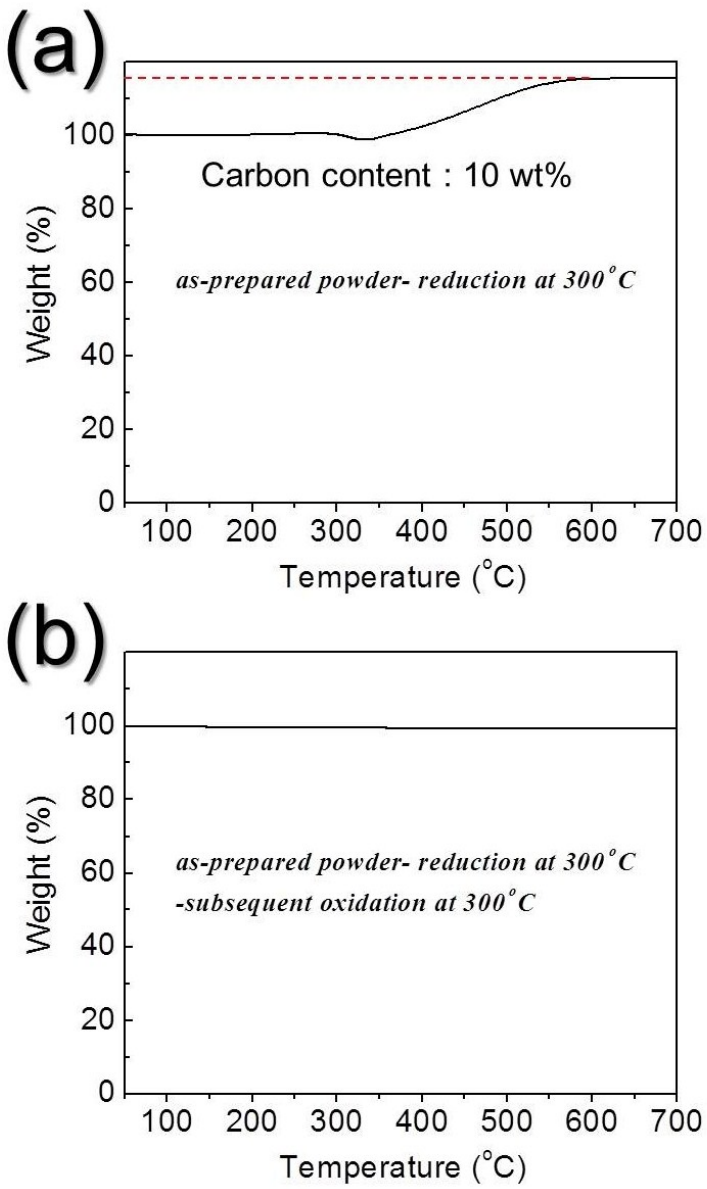

Fig. S4. TG curves of the (a) Ni-C composite powders obtained by reduction process at 300 °C under 10% H_2/Ar gas and (b) hollow NiO aggregates obtained by oxidation of the reduced Ni-C composite powders at 300 °C under air.

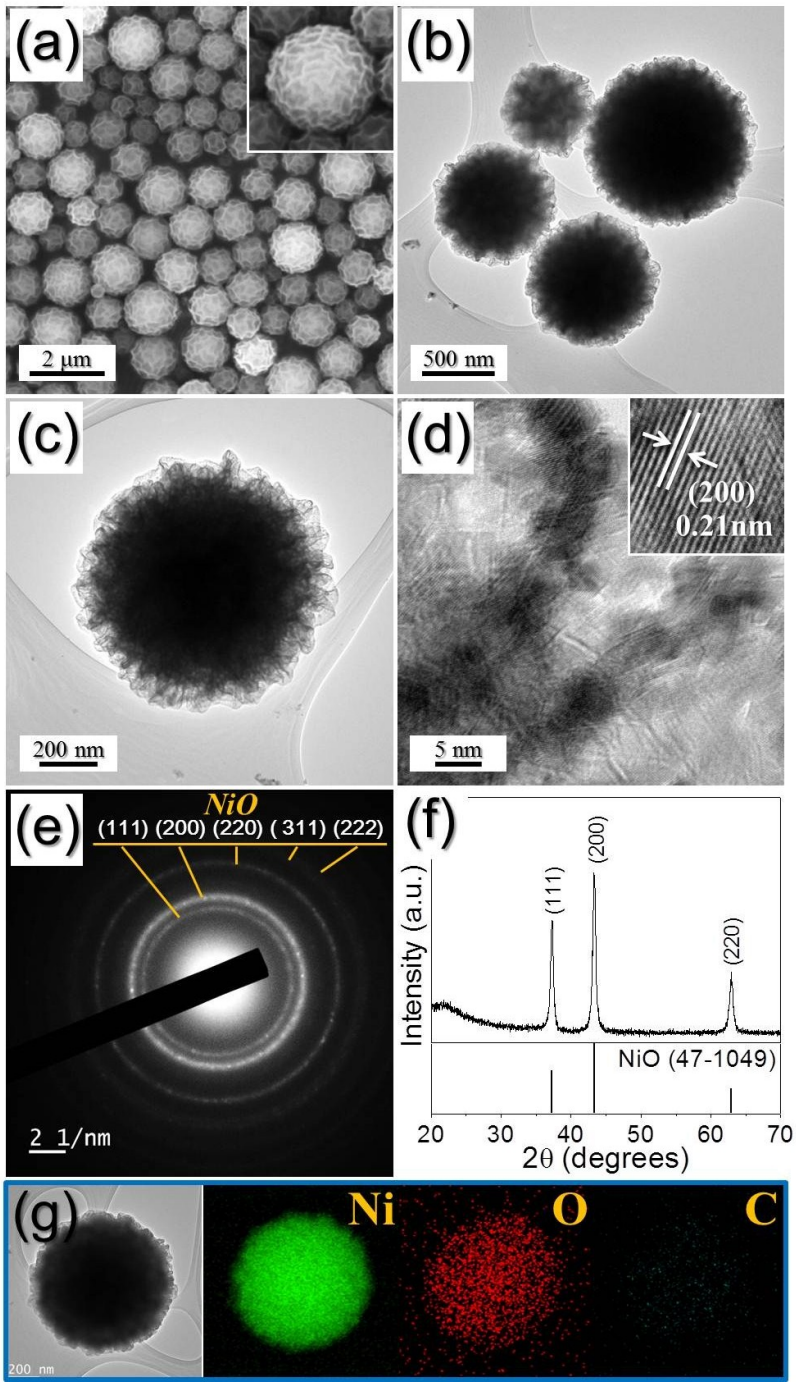

Fig. S5 Morphologies, SAED pattern, XRD pattern, and elemental mapping images of the solid NiO aggregates obtained by direct oxidation of as-prepared precursor powders at 300 ^{o}C under air: (a) SEM, (b, c) TEM images, (d) HR-TEM image, (e) SAED pattern, (f) XRD pattern, and (g) elemental mapping images.

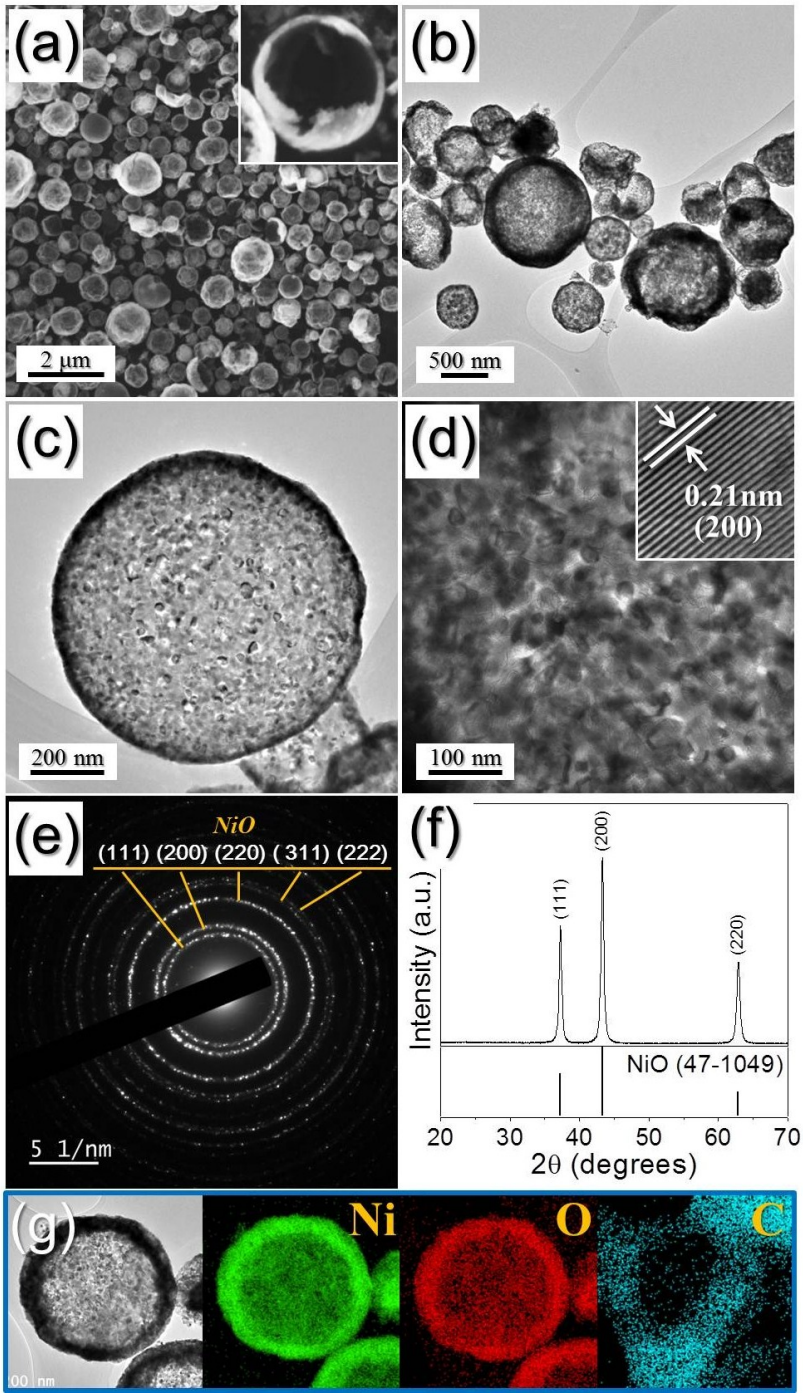

Fig. S6 Morphologies, SAED pattern, XRD pattern, and elemental mapping images of the hollow NiO shell obtained by spray pyrolysis: (a) SEM, (b, c) TEM images, (d) HR-TEM image, (e) SAED pattern, (f) XRD pattern, and (g) elemental mapping images.

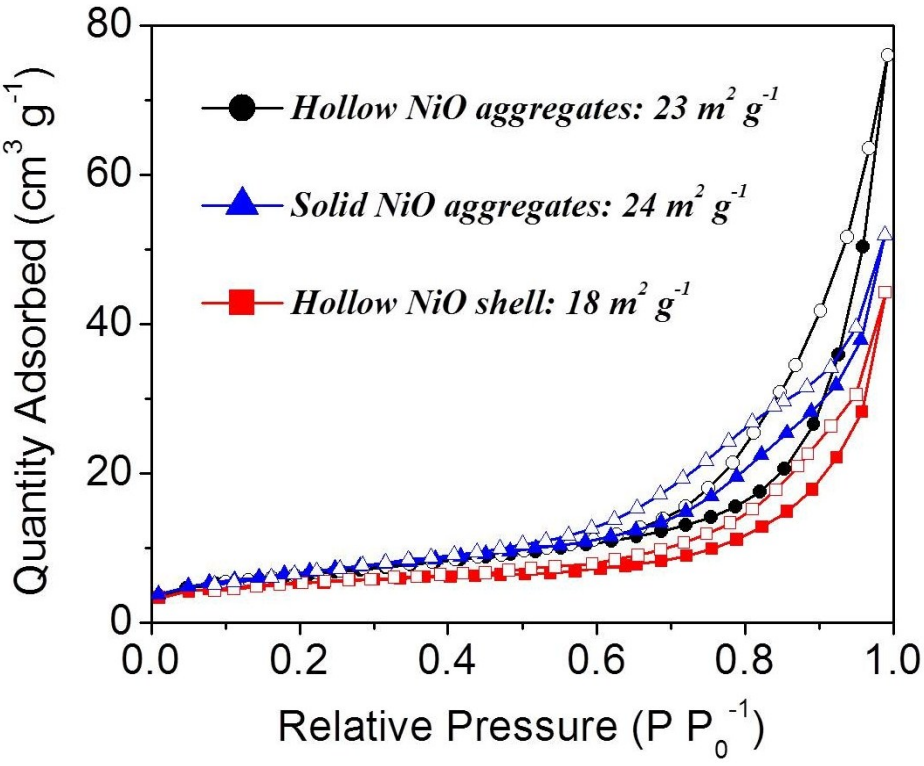

Fig. S7. N_2 adsorption-desorption isotherms measured at 77 K for the hollow NiO aggregates, which were formed through the synergetic effects of nanoscale Kirkendall diffusion and Ostwald ripening, and solid NiO aggregates and hollow NiO shell.

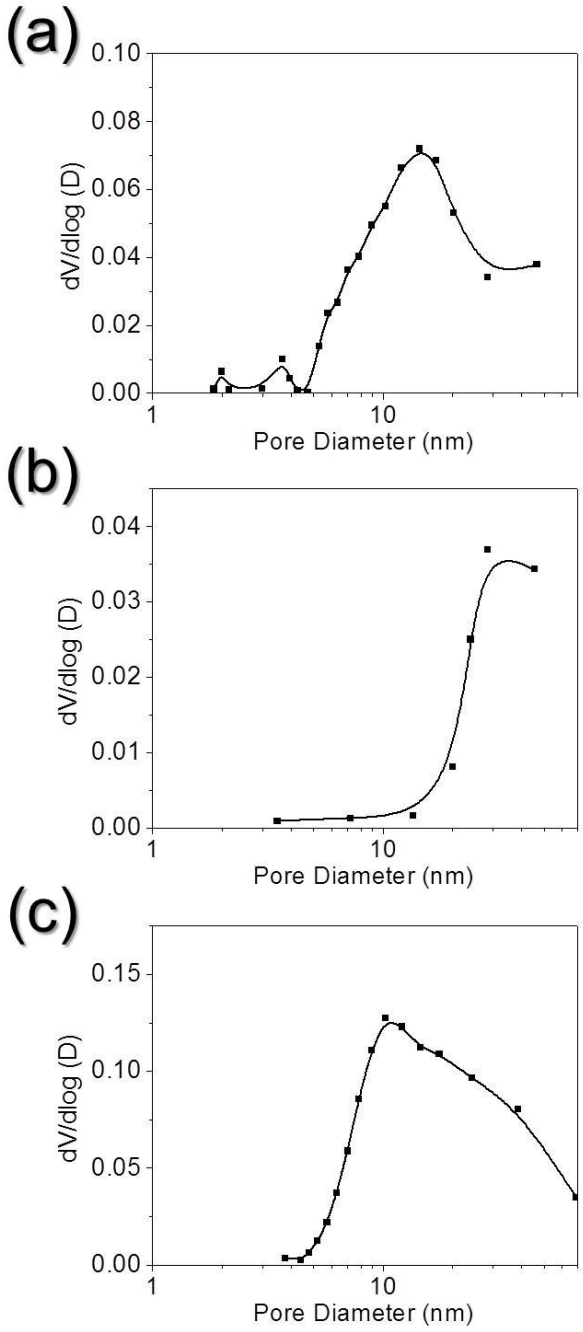

Fig. S8. Pore size distributions of (a) hollow NiO aggregates, (b) solid NiO aggregates and (c) hollow NiO shell.

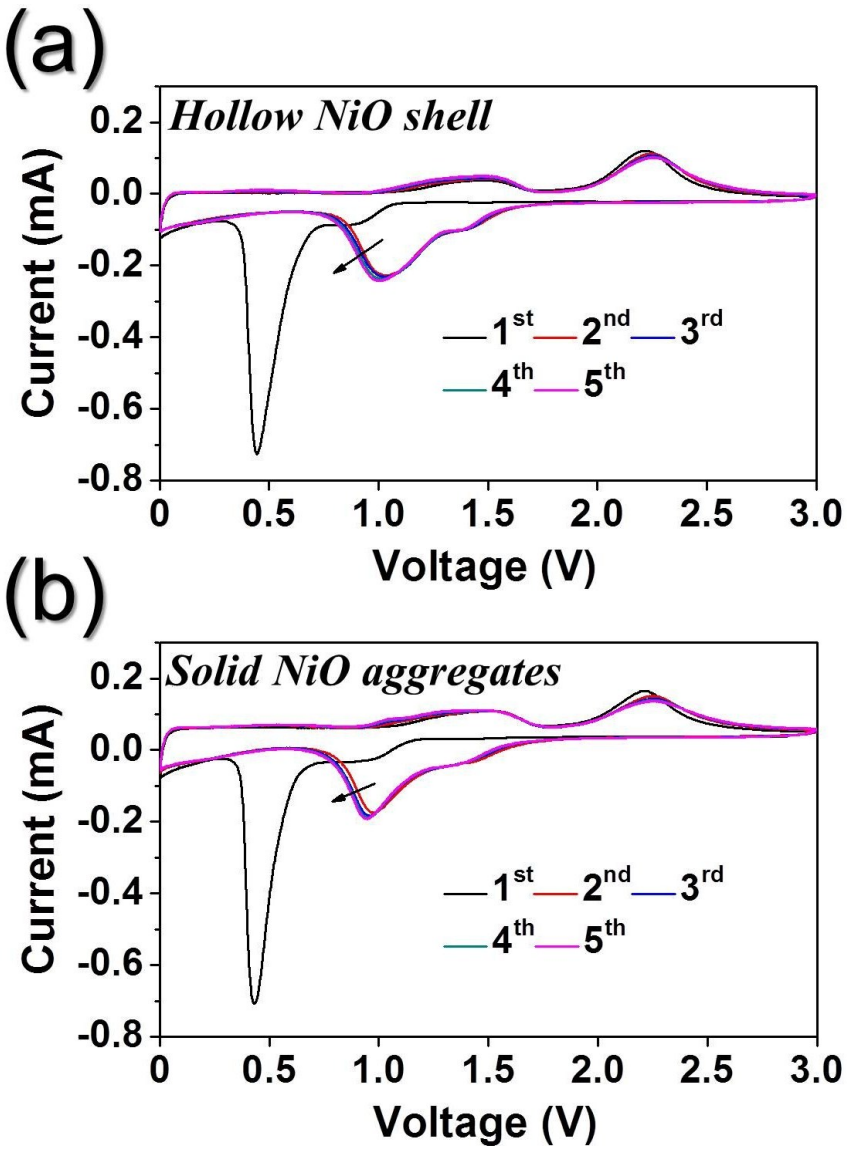

Fig. S9. Cyclic voltammogram (CV) curves of the (a) hollow NiO shell and (b) solid NiO aggregates for the first 5 cycles at a constant current density of 1.0 A g^{-1}.

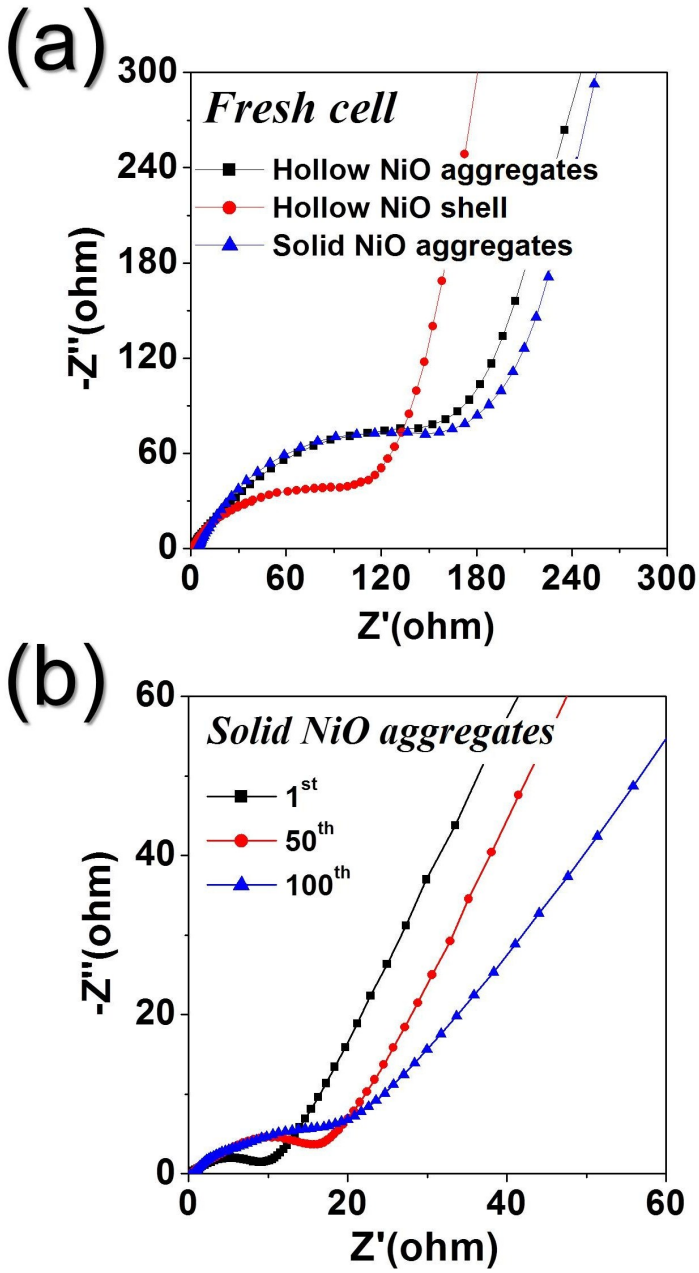

Fig. S10. Nyquist impedance plots of the (a) three samples before cycling and (b) solid NiO aggregates after cycling.

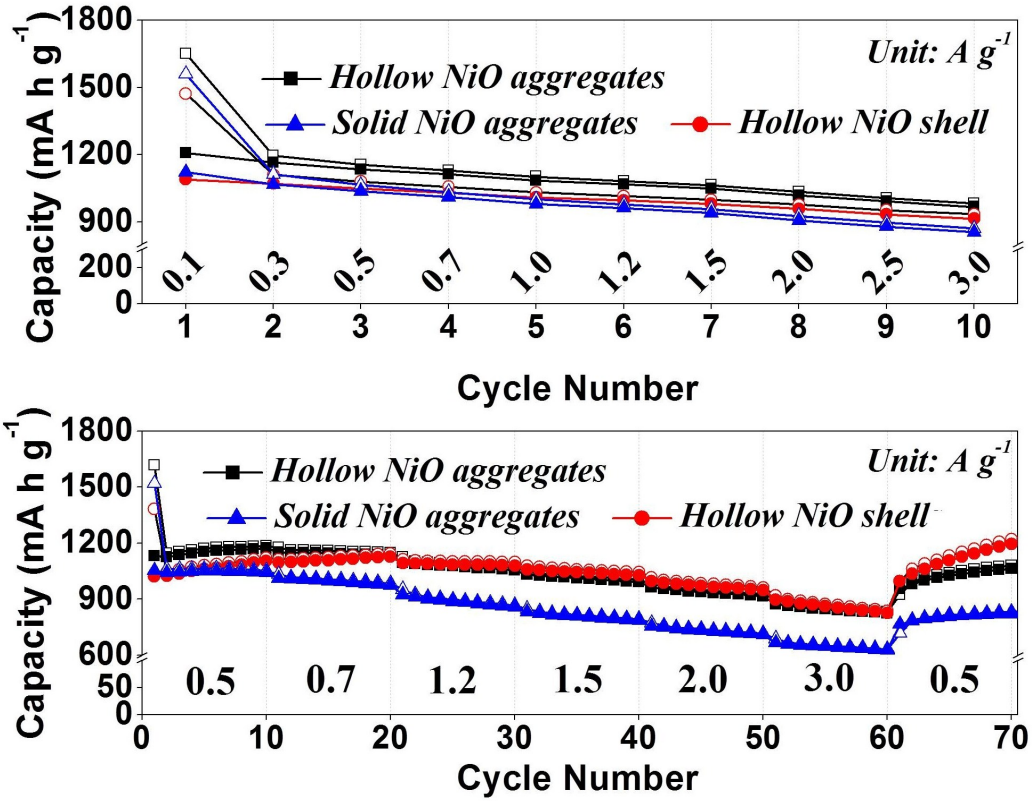

Fig. S11. Rate performances of the hollow NiO aggregates, which were formed through the synergetic effects of nanoscale Kirkendall diffusion and Ostwald ripening, and solid NiO aggregates and hollow NiO shell.

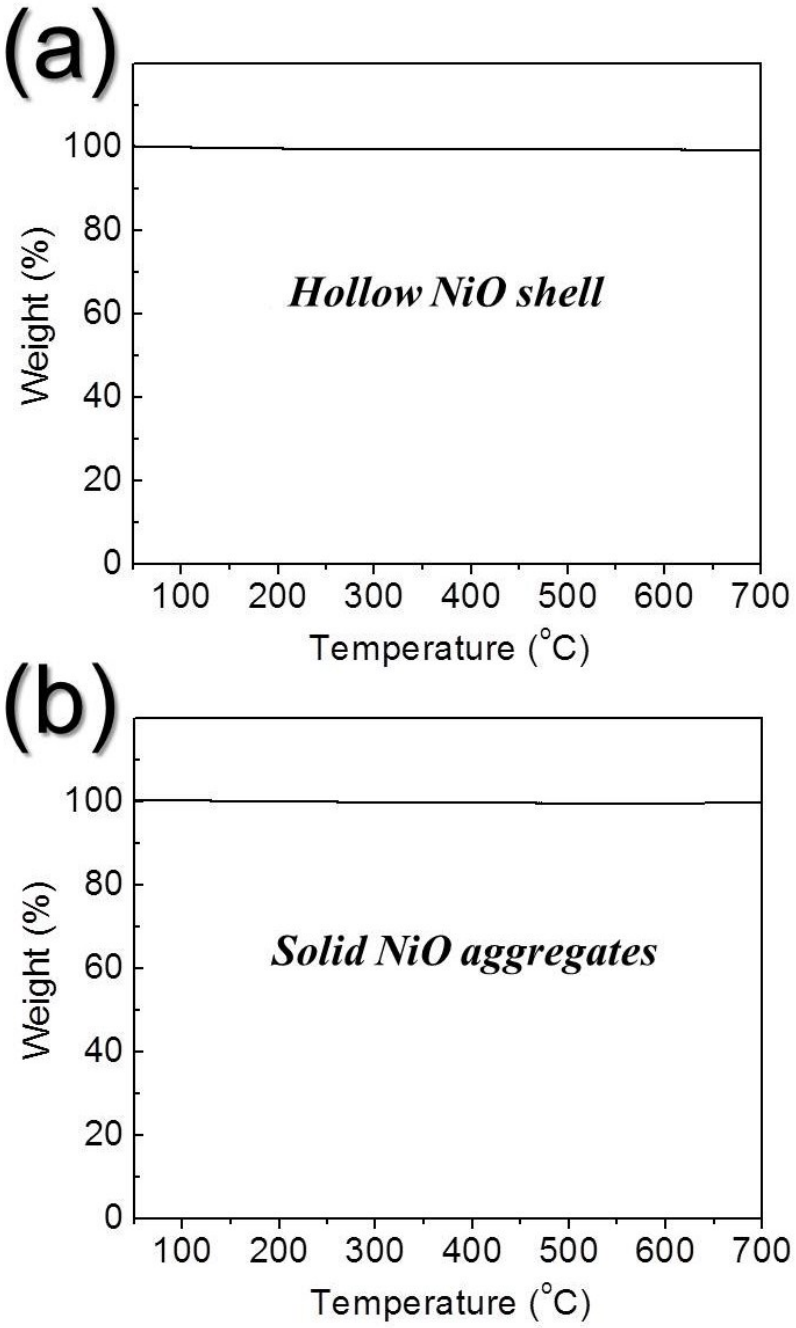

Fig. S12. TG curves of the (a) hollow NiO shell and (b) solid NiO aggregates.

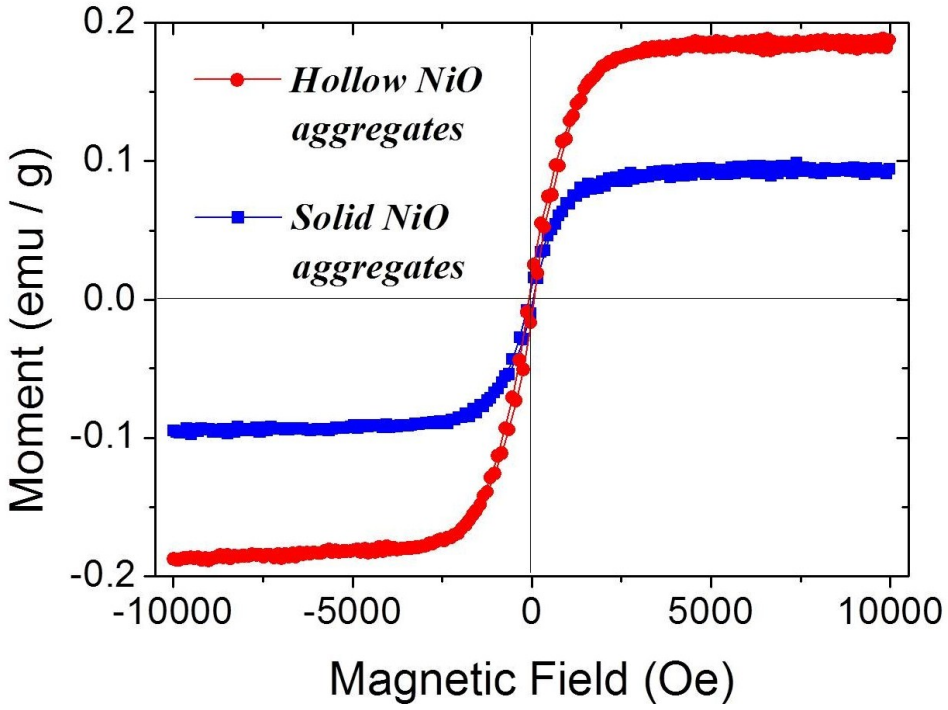

Fig. S13. Hysteresis curves of the hollow NiO aggregates and solid NiO aggregates.

Table S1. Comparison of the electrochemical performances of the hollow NiO aggregates formed through the synergetic effect of nanoscale Kirkendall diffusion and Ostwald ripening with the reported results of the nanostructured nickel oxide materials.

Materials	Voltage range (V)	Current rate	Initial C_{dis}/C_{cha} [mA h g^{-1}]	Discharge capacity [mA h g^{-1}]	Cycle number	Ref.
spherical and hollow-structured NiO aggregates	**0.001-3**	**1000 mA g^{-1}**	**1543/1099**	**1118**	**500**	**In this work**
NiO nanofibers	0.005-3	80 mA g^{-1}	~1280/~784	~583	100	S1
NiO microspheres	0.01-3	100 mA g^{-1}	1570/~1060	100	30	S2
NiO nanowall	0.005-3	895 mA g^{-1}	1050/833	~638	85	S3
NiO nanoshafts	0.01-3	50 mA g^{-1}	1300/~860	410	30	S4
NiO/RuO_2 composite carbon nanofibers	0.005-3	40 mA g^{-1}	~650/~480	360	40	S5
NiO/MWCNT	0.05-3	50 mA g^{-1}	1084/720	800	50	S6
NiO@TiO_2 core-shell nanopowders	0.001-3	300 mA g^{-1}	1302/937	970	80	S7
porous NiO fiber	0.01-3	40 mA g^{-1}	~1100/696	~638	50	S8
NiO hollow microspheres	0.02-3	100 mA g^{-1}	1100/620	560	45	S9
NiO/grapheme	0.02-3	100 mA g^{-1}	~1100/~730	646	35	S10
NiO-C nanocomposite	0.01-3	700 mA g^{-1}	1102/1002	382	50	S11
NiO yolk-shell powders	0.001-3	700 mA g^{-1}	~1200/898	951	150	S12
NiO nanoflake arrays	0.01-3	100 mA g^{-1}	900/~750	720	20	S13
Co-doped NiO nanoflake	0-3	100 mA g^{-1}	1201/882	600	50	S14
Co-doped NiO nanoparticles	0-3	71.8 mA g^{-1}	1301/1006	1018	50	S15
3D flower-like NiO	0.01-3	100 mA g^{-1}	1496/1186	713	40	S16
bamboo-like amorphous carbon nanotubes clad in ultrathin NiO nanosheets	0.01-3	800 mA g^{-1}	1377/936	1034	300	S17

References

S1 V. Aravindan, P. Suresh Kumar, J. Sundaramurthy, W. C. Ling, S. Ramakrishna,

S. Madhavi, *J. Power Sources,* 2013, **227**, 284-290.

S2 L. Liu, Y. Li, S. Yuan, M. Ge, M. Ren, C. Sun, Z. Zhou, *J. Phys. Chem. C,* 2010, **114**, 251-255.

S3 B. Varghese, M. V. Reddy, Z. Yanwu, C. S. Lit, T. C. Hoong, G. V. S. Rao, B. V. R. Chowdari, A. T. S. Wee, C. T. Lim, C. H. Sow, *Chem. Mater*., 2008, **20**, 3360-3367.

S4 L. Yuan, Z. P. Guo, K. Konstantinov, P. Munroe, H. K. Liu, *Electrochem. Solid-State Lett*. 2006, **9**, A524-A528.

S5 Y. Wu, R. Balakrishna, M. V. Reddy, A. S. Naira, B. V. R. Chowdari, S. Ramakrishna, *J. Alloys Compd.,* 2012, **517**, 69-74.

S6 C. Xu, J. Sun, L. Gao, *J. Power Sources,* 2011, **196**, 5138-5142.

S7 S. H. Choi, J. H. Lee, Y. C. Kang, *Nanoscale,* 2013, **5**, 12645-12650.

S8 B. Wang, J. L. Cheng, Y. P. Wu, D. Wang, D. N. He, *Electrochem. Commun*., 2012, **23**, 5-8.

S9 D. Xie, W. Yuan, Z. Dong, Q. Su, J. Zhang, G. Du, *Electrochim. Acta,* 2013, **92**, 87-92.

S10 Y. J. Mai, S. J. Shi, D. Zhang, Y. Lu, C. D. Gu, J. P. Tu, *J. Power Sources,* 2012, **204**, 155-161.

S11 M. M. Rahman, S. L. Chou, C. Zhong, J. Z. Wang, D. Wexler, H. K. Liu, *Solid State Ionics,* 2010, **180**, 1646-1651.

S12 S. H. Choi, Y. C. Kang, *ACS Appl. Mater. Interfaces,* 2014, **6**, 2312-2316.

S13 H. Wu, M. Xu, H. Wu, J. Xu, Y. Wang, Z. Peng, G. Zheng, *J. Mater. Chem.,* 2012, **20**, 19821-19825.

S14 Y. J. Mai, J. P. Tu, X. H. Xia, C. D. Gu, X. L. Wang, *J. Power Sources,* 2011, **196**, 6388-6393.

S15 T. V. Thi, A. K. Rai, J. H. Gim, J. K. Kim, *J. Power Sources,* 2015, **292**, 23-30.

S16 Q. Li, Y. Chen, T. Yang, D. Lei, G. Zhang, L. Mei, L. Chen, Q. Li, T. Wang, *Electrochim. Acta,* 2013, **90**, 80-89.

S17 X. Xu, H. Tan, K. Xi, S. Ding, D. Yu, S. Cheng, G. Yang, X. Peng, A. Fakeeh, R. V. Kumar, *Carbon,* 2015, **84**, 491-499.